AIAA JOURNAL
Vol. 42, No. 10, October 2004

Enhanced Evaluation of the Low-Velocity Impact Response of Composite Plates

Paolo Feraboli* and Keith T. Kedward†
University of California, Santa Barbara, Santa Barbara, California 93106

Recent research programs conducted on low-velocity impact events on composite structures have used force as the sole governing parameter and based their damage resistance and tolerance considerations on the peak recorded value. Understanding of other available parameters, such as contact duration and coefficient of restitution, which are related to the effective structural stiffness of the target, is fundamental in the design of a methodology for assessing impact performance and can offer greater insight in the interpretation of future research programs. An experimental database is gathered through drop tower impact testing by means of a rigid striker on clamped circular plates, for a particular polymer composite system. Several researchers have presented data showing that a critical value of the impact force for the onset of damage exists. Structural properties are hereby studied in both the sub- and supercritical regimes, which means for impact energy values below and above the damage threshold. A modified approach to the classic spring–mass model, which employs the notions of damaged stiffness and dissipated energy, leads to the derivation of approximate formulas that describe the peak force-energy curve. In particular, the introduction of a dashpot to simulate the effect of damage greatly improves the accuracy of the model in the regime beyond the structural integrity threshold. A novel method to assess the residual performance of the damaged plate is developed, and it consists in low-energy, nondestructive impact testing, the results from which bear a striking resemblance with the curves obtained by compression after impact.

I. Introduction

IMPACT tests can prove inherently difficult to understand because of the large number of parameters that play a key role in such events, particularly in the case of laminated composite structures due to their heterogeneous anisotropic nature and the complex failure modes that can occur. The current experimental investigation is conducted on square plates, supported over circular openings, having a quasi-isotropic $[0/90/\pm45]_{4s}$ stacking sequence. Such a configuration benefits from the axial symmetry of the circular geometry and the low degree of anisotropy of the laminate and thus facilitates the concentration on the mechanics of the impact event and the complex failure mechanisms.

An extensive literature review has indicated that many questions still surround the impact response of composite plates. In particular, an ongoing debate exists on whether force or energy should be used to compare impact test results on different configurations, as well as whether a force- or energy-based criterion should be employed to predict the structural integrity threshold or uniquely and satisfactorily assess the state of damage in the plate. The aim of this paper is to show how governing parameters, such as force, energy, and structural stiffness vary between the subcritical and supercritical regimes and that peak force, although extremely valuable for predicting the damage threshold, cannot be used independently for investigating the impact performance of a composite structure.

The use of an instrumented drop tower such as the General Research Corp. (GRC) Dynatup© enables the recording of force and time, which are directly measured, as well as energy, deflection, and velocity, which are calculated. Using a conventional experimental setup derived from the suggested ASTM International Standard D6264[1] and shown in Fig. 1, it is possible to characterize the elastic behavior, failure initiation, and failure propagation in terms of applied dynamic force and energy. To understand the transition from quasi-static to low-velocity impact, the same test fixture and geometry used for impact testing is used to assess the static behavior of the plate.

Although load vs deflection data for a static test are sufficient to characterize fully the response of a structure or a material, an impact test requires not only additional information to indicate the severity of the event, but also a deep understanding of how certain parameters interact to influence the results. The load-deflection curve typically used to describe a static test, such as that shown in Fig. 2, can be characterized by the value of incipient failure [1656 lb (7366 N)], which corresponds to the first significant drop in the loading curve, and by the value of ultimate load [2541 lb (11,303 N)], beyond which the structure's ability to carry additional load is compromised. These values depend strictly on material properties and test geometry and, for modern epoxy systems, are independent of the speed at which the test is performed, in the range of static testing (0.01–0.1 in./min; 0.25–2.54 mm/min).

A force–time trace, such as Fig. 3a, or, equivalently, the load-deflection curve of Fig. 2, can exhibit separate values for critical and peak force values at sufficiently high-impact energy levels (supercritical test). At lower impact energy values, near the delamination threshold, the values of critical and peak force coincide (critical test), whereas at even lower values they lose significance, in the sense that failure does not occur and peak force is just an indication of the response to an elastic impulse (subcritical). To facilitate the understanding of these concepts, a brief summary of the terminology used is reported:

1) Impact energy is the impactor's incident kinetic energy.

2) Peak force is the maximum recorded force.

3) Critical force is the value of the force at which a first change in out-of-plane stiffness of the material occurs; it is also denoted as delamination threshold.

4) Critical energy is the value of the impact energy corresponding to the critical force.

5) Dissipated energy is the amount of energy absorbed mainly in damage mechanisms but also in other nonconservative phenomena, that is, vibrations, friction, specimen/fixture slipping, and, therefore, not restituted to the rebounding impactor.

Received 13 August 2003; presented as Paper 2004-1841 at the AIAA 45th Structures, Structural Dynamics, and Materials Conference, Palm Springs, CA, 19–22 April 2004; revision received 4 May 2004; accepted for publication 10 May 2004.

*Research Assistant, Department of Mechanical Engineering; pmc@engineering. ucsb.edu. Student Member AIAA.

†Professor, Department of Mechanical Engineering. Fellow AIAA.

6) Coefficient of restitution is the ratio of exit to impact velocity or, equivalently, the ratio of the square root of exit to impact energy.

7) Total contact duration is the resident time of the impactor on the target.

8) Subcritical (or elastic) impact events are the range of impact energy values below damage threshold.

9) Supercritical impact events are the range of impact energy values above threshold.

10) Mean static failure load (MSFL) is the load corresponding to the onset of delamination during quasi-static testing.

11) Mean static ultimate load (MSUL) is the maximum recorded load during quasi-static testing.

Failure is here defined as a sharp drop in the load-time curve, corresponding to damage initiation, either in the ply plane or at the interface of two adjacent plies. The nature of in-plane failure is either matrix splitting or fiber breakage, whereas the nature of interply failure is delamination induced by interlaminar shear. It is known that structural failure in composite materials can occur by internal delaminations without evident external fracture surfaces.

II. Literature Review

Numerous studies on low-velocity impacts performed by means of drop tower testing have been conducted on analogous carbon/epoxy composite systems with quasi-isotropic stacking sequences and either circular or square plates. Jackson and Poe's[2] and Sjöblom's[3] early work suggested that impact force and not energy should be used as the key parameter to describe the damage response of composite targets. They also conclude that impact energy is not the controlling parameter for failure threshold; rather it is the impact force, indicating the existence of a critical force, which is a constant of the structure, independent of plate size and boundary conditions.

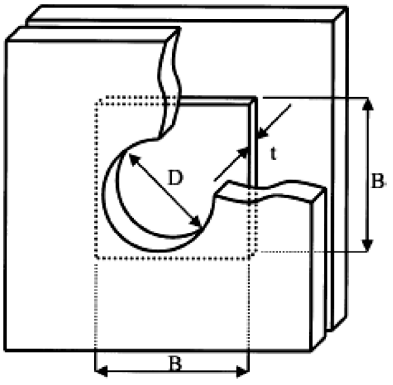

Fig. 1 Impact and static loading fixture, from Ref. 25: $D = 2.5$ in. (63.5 mm), $B = 5$ in. (127 mm), and $t = 0.145$ in. (3.68 mm).

Earlier work by Aleszka[4] showed that a threshold impact energy value exists, that it corresponds to a precise value of the contact force, and that both are independent of impact energy beyond failure initiation. He also realized that peak force does not increase monotonically with impact energy after initiation of damage, but it rapidly reaches an asymptotic value. More recently, Belingardi and Vadori[5] recognized the difference between critical and peak force and plotted the two values to show their independence from impact energy after the onset of damage, but they failed to investigate the behavior below such threshold. Delfosse and Poursartip[6] pointed out that, although force should be used as controlling parameter up to the onset of damage, its use in the creation of damage maps to quantify the extent of damage is not recommended.

Nettles and Douglas[7] based their parametric investigation on the peak force obtained from testing different targets at different values of impact energy. Comparisons were performed on the total delamination area and plotted vs contact force for various values of incident kinetic energy.

Hahn et al.[8] and Cartie and Irving[9] reported that residual strength depends on the state of damage within the plate and plotted the damage area and the normalized compression after impact (CAI) strength against the impact energy. Schoeppner and Abrate[10] observed the distinction between critical and peak force and introduced the concept of normalized peak force, obtained dividing the peak force by the critical force, to eliminate the peak force variability with impact energy.

Ambur and Kemmerly[11] plotted peak force and damage area vs impact energy and reported unpredictable trends in the results, such as the plots for the 10-lb (4.54-kg) impactor. Ambur and Starnes[12] plotted the peak contact force against shell curvature, having indicated plates as shells with a 200-in. (5080-mm) radius of curvature. They used a constant value of impact energy, required for the onset of barely visible impact damage (BVID) and reported nonlinear behaviors. In other publications,[13–17] however, the parametric investigations were based on peak force recorded at the same impact energy level; therefore, more consistent results were obtained.

Zhou[18,19] for glass/polyester and glass/phenolic composites, Found and Howard[20] for woven carbon/epoxy laminates, and Scarponi et al.[21] for tape and woven carbon/epoxy face-sheets sandwich plates reported peak force–impact energy curves that asymptotically tend to the laminate's ultimate load bearing capability. Liu and Raju[22] performed a series of tests on cross-ply glass–epoxy laminates and used a multiparameter methodology to interpret the results and determine the perforation threshold of their targets. The contact duration plot showed a quadratic increase up to perforation, followed by a sharp drop. The CAI tests revealed that the normalized maximum load decreases from unity (undamaged value) to about 50% at perforation, where it plateaus even at higher impact energy levels.

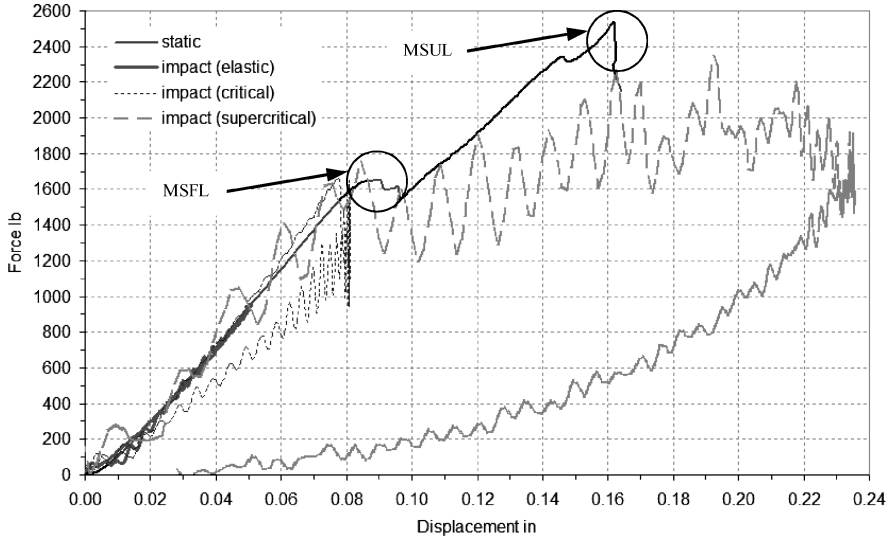

Fig. 2 Comparison of static and impact load vs displacement curves.

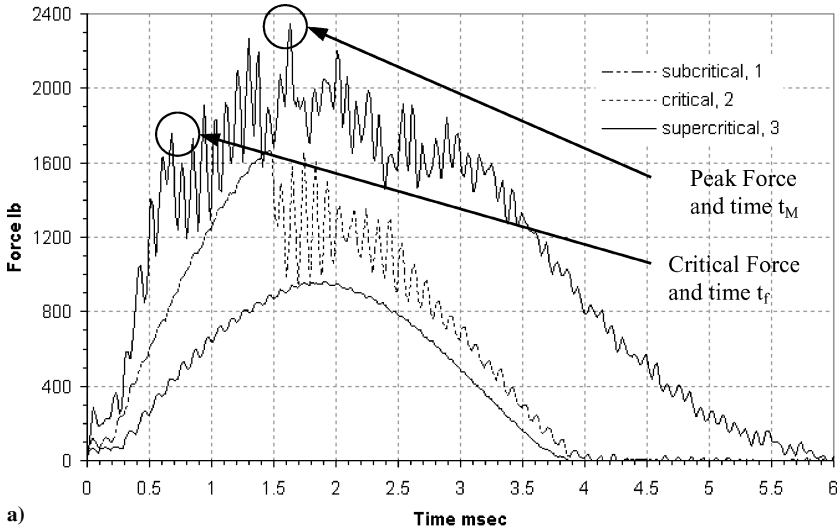

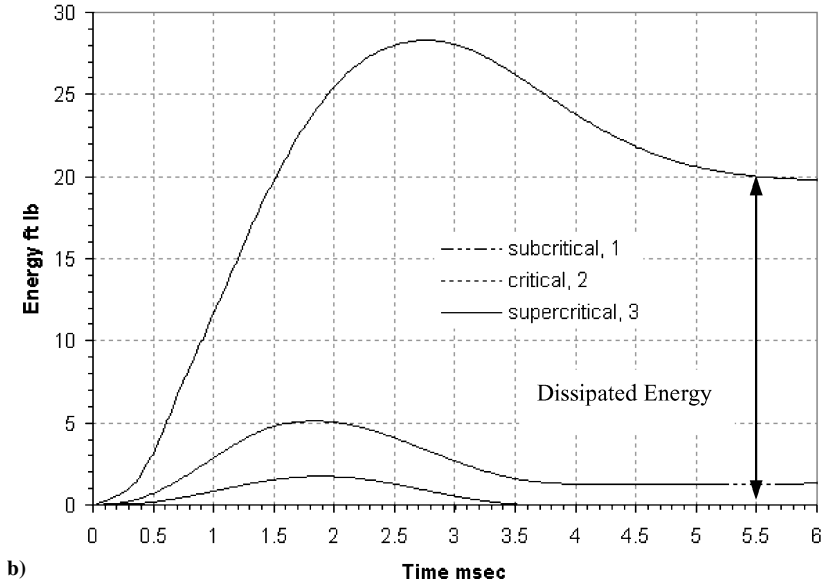

Fig. 3 Force and energy vs time for subcritical, critical, and supercritical impact events.

In their investigation on quasi-isotropic beam specimens, Lifschiz et al.[23] introduced the concept of a three-test sequence to determine the pristine and damaged values of transverse stiffness. The first and third subcritical tests are employed to record total contact duration, which is directly related to effective structural stiffness, whereas the second critical test is used to introduce damage in the structure. They quantified the residual performance of their beam targets by means of relative loss in impact energy, which is linearly related to the relative reduction in beam rigidity.

III. Specimen Fabrication and Test Setup

The laminates used are obtained by hand layup of carbon/epoxy AS4/NCT301 prepreg tape, then are press molded at 300°F (149°C) for 30 min at a pressure of 3 bar (43.5 psi). The stacking sequence is quasi isotropic of the form $[0/90\ \text{deg}/\pm 45]_{4s}$, with a nominal ply thickness of 0.0045 in. (0.11 mm), giving nominal laminate thickness of 0.145 in. (3.68 mm). The unidirectional lamina and quasi-isotropic laminate properties are summarized in Ref. 24. From the cured 12×12 in. (304.8×304.8 mm) panel, four square plates of nominal length of 5 in. (127 mm) are cut with a diamond-coated tip disk saw. The fixture (Fig. 1, from Ref. 25) comprises two steel plates 0.5 in (12.7 mm) thick, having a 2.5-in. (63.5-mm)-diam circular opening, clamped by means of four peripheral screws. The composite plate is situated between the two steel plates and is positioned over the aperture with the aid of three locating pins. The instrumented drop tower is a GRC Dynatup Model 8250, and data acquisition is performed on a personal computer with the 930 software package. For the present study, the impactor carriage weight is kept constant at 9.92 lb (4.5 kg) and the striker or tup is machined from a 6061-T6 aluminum cylinder with a 1.5-in. (38.1-mm)-diam hemispherical end. Maximum impact energy is 56 ft · lb (75.92 J); such a range covers the entire range of low- and medium-threat impact events as well as the majority of the high-threat events, as indicated by Kan et al.[26] and Kan.[27] This particular structural configuration (recapitulated in Table 1) is chosen because of the large experimental database available, but the same observations have been reported for other configurations.[28] To show the applicability of the results derived in the following sections to other configurations, the results obtained for three other values of laminate thickness (16, 24, and 40 plies) and one value of support span (5-in. diam) are also summarized. More extensive considerations may be found in Ref. 28, where laminate thickness, aperture diameter, impactor weight and diameter, impact velocity and energy, average in-plane laminate modulus, and boundary conditions are varied experimentally and analytically between a wide range of configurations.

Static testing is performed on an Instron 1123 electromechanical, double-screw test frame under displacement control using the same fixture employed in the impact testing. Damage evaluation is performed with a Krautkramer–Branson CL304 ultrasonic A-scan, with has a single probe that functions in a pulse-echo mode, and via

a Nikon EPIPHOT 200 for optical-microscopy image analysis after cross sectioning and polishing of the specimens.

IV. Results and Discussion

A. Force and Energy Curves

The peak force recorded by testing at different values of impact energy is shown in Fig. 4a. The Fig. 4a plot is divided in two regions by the critical force and corresponding impact energy level, namely, the subcritical and supercritical regimes, according to whether detectable damage is introduced. The average load value of 1750 lb (7784 N) recorded at the threshold, defined as critical force, appears to be slightly higher than the quasi-static MSFL of 1656 lb (7366 N), but the discrepancy can be attributed to the inertial oscillations associated with the dynamics of the event. The critical force value has been previously shown to be constant with increasing impact energy.[2–5,9,10,25]

Table 1 Summary of experimental setup

Parameter	Value
Material	AS4/NCT 301
Stacking sequence	$[0/90/\pm45]_{4s}$
Number of plies	32
Nominal thickness, mm (in.)	3.68 (0.145)
Shape	Pseudocircular
Arperture diameter, mm (in.)	63.50 (2.5)
Boundary condition	Pseudoclamped
Impactor diameter, mm (in.)	38.10 (1.5)
Impactor mass, kg (lb)	4.50 (9.92)

When a spring–mass model[29,30] is used,

$$m\ddot{x} + K_0 x = 0 \tag{1}$$

$$P = -m\ddot{x} \tag{2}$$

it is possible to obtain the known sine function

$$x = V \cdot \sqrt{K_0 m} \cdot \sin\left(\sqrt{K_0/m}\, t\right) \tag{3}$$

If the assumption of linear elastic response is made,

$$U = \tfrac{1}{2} P^{\text{peak}} \cdot x^{\text{peak}} \tag{4}$$

the data for the peak force can then be accurately fitted by the well-accepted power law curve[29]:

$$P_{\text{th}}^{\text{peak}} = \sqrt{2 \cdot K_0 \cdot E_i} \tag{5}$$

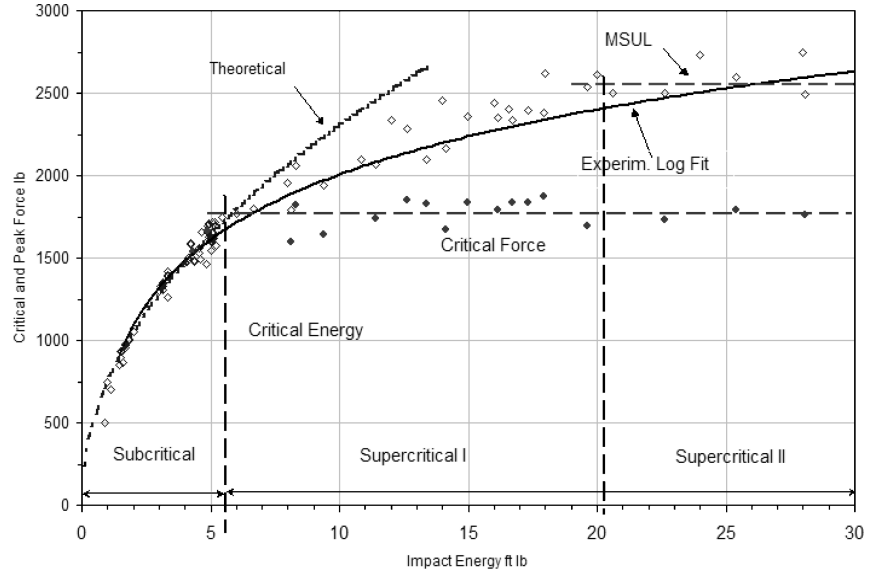

a)

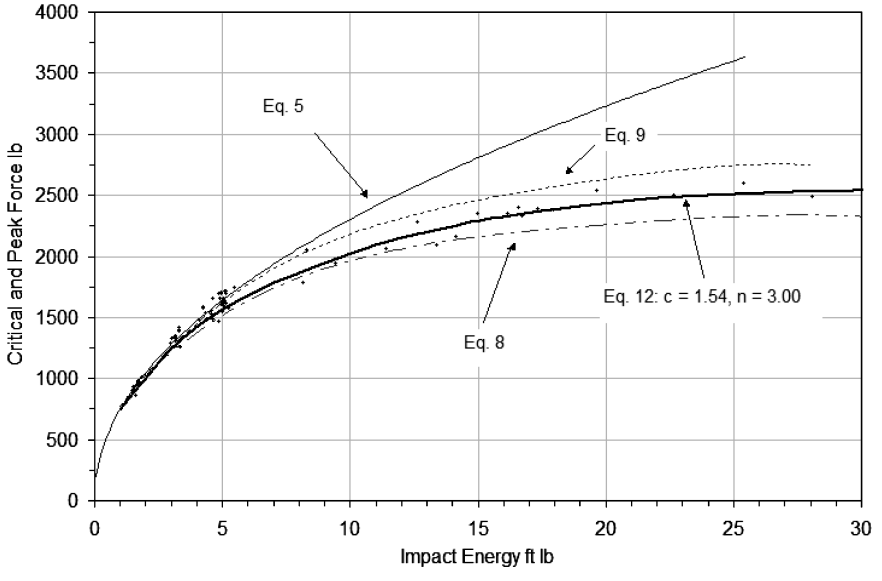

b)

Fig. 4 Peak and critical force dependence on impact energy: a) experiments and b) models.

where m is impactor mass, U is the strain energy, equivalent to the impact energy E_i, P and P^{peak} are the instantaneous and peak force, K_0 is the undamaged structural stiffness, V is the impact velocity, and x is the transverse displacement of the carriage, which is assumed to coincide with the target, hence, assuming that there is no significant permanent indentation.

Although the power law of Eq. (5) predicts an unbounded increase of the peak force, because it is based on the assumption of a purely elastic system, the experimental data show that it deviates from this theoretical value as damage accumulates and asymptotically but quickly reaches a plateau. Notice that this asymptotic value coincides with the laminate's quasi-static MSUL of 2541 lb (11,303 N) (Refs. 4 and 19).

A rigorous approach in describing the peak force curve after the introduction of damage imposes an account of the progressive change in transverse stiffness throughout the duration of the impact event, associated with the instantaneous state of damage. Because the instantaneous value of the structural stiffness K_j^D is a function of both time and available kinetic energy, a more general equation could have the form

$$P_{\text{real}}^{\text{peak}} = \left\{ 2 \cdot \left[K_0 \left(\frac{t_{f1}}{t_M} \right) + K_1^D \left(\frac{t_{f2} - t_{f1}}{t_M} \right) + \cdots + K_j^D \left(\frac{t_M - t_{M-1}}{t_M} \right) \right] \cdot E_i \right\}^{\frac{1}{2}} \tag{6}$$

where $t_{f1}, t_{f2}, \ldots, t_{fi}$ are times to first, second, $\ldots$, ith failure and t_M is the time to peak force.

Because peak force is reached at the peak of the load–time curve, it is fair to assume that only the loading part of the curve up to t_M contributes to reaching that value. For an elastic event then, where failure does not occur, time to failure equals time to peak force; hence, Eq. (6) reduces to Eq. (5). In the case of a supercritical event, as the one described by curve 3 in Fig. 3a, where one drop in the load–time curve is clearly distinguishable, Eq. (6) becomes

$$P_{\text{real}}^{\text{peak}} = \sqrt{2 \cdot \left\{ K_0 (t_{f1}/t_M) + K_1^D [(t_M - t_{f1})/t_M] \right\} \cdot E_i} = \sqrt{2 \cdot \left[K_0 (0.41) + K_1^D (0.59) \right] \cdot E_i} \tag{7}$$

because $t_{f1} = 0.7$ ms and $t_M = 1.7$ ms. The dimensionless time terms give a quantification (percentage) of the individual contributions that the instantaneous stiffness values have on reaching the peak force.

To compensate for the extensive experimental correlation as well as the computational accuracy that this new equation requires, a simplified model can be employed, which assumes that, from the onset of damage on, the energy dissipated in the fracture process does not contribute to increasing the peak recorded force. When the energy dissipated during the fracture process E_D is introduced, it is possible to obtain

$$P_1^{\text{peak}} = \sqrt{2 \cdot K_0 \cdot (E_i - E_D)} \tag{8}$$

This simple, novel equation assumes that initiation and propagation of damage has the effect of reducing the amount of energy available for structural response, hence for the ability to reach the theoretical peak force. The onset of damage effectively reduces the amount of available kinetic energy by absorbing part of it during the fracture process. This equation tends to underestimate the actual value of the peak force, as can be seen in Fig. 4b, because only part of the damage process occurs during the loading part of the curve, whereas the other part of it occurs at and after reaching peak force. Therefore, subtracting the whole amount of dissipated energy before reaching peak force tends to be a nonconservative assumption.

A different approach accounts for the fact that, at higher impact energy values, failure occurs at an earlier stage in the load vs time curve, and the pristine structural stiffness K_0 is assumed to be related to the impact energy E_i up to time to failure t_f, whereas for the remaining part of the impact event $(t_M - t_f)$ up to peak force to the difference between impact energy and dissipated energy E_D:

$$P_2^{\text{peak}} = \sqrt{2 \cdot K_0 \cdot \{E_i (t_f/t_M) + [(t_M - t_f)/t_M] \cdot (E_i - E_D)\}} = \sqrt{2 \cdot K_0 \cdot \{E_i - [(t_M - t_f)/t_M] \cdot E_D\}} \tag{9}$$

where the assumption that the energy absorbed in the damage process does not contribute to the elastic response of the structure still holds. Whereas Eq. (9) manages to captures the asymptotic behavior of the experimental data, it tends to overestimate the actual value of the peak force because the amount of energy being dissipated is not zero in the time range up to failure (t_f/t_M), as shown in Fig. 4b. The best fit to the experimental data can be obtained by means of a logarithmic function,[24] which captures the tendency of the curve to deviate from the power law curve toward an asymptotic value[18–21] and provides an acceptable approximation in the elastic regime, as shown in Fig. 4a. If damage is interpreted as a nonlinear viscous damper, proportional to a power of the impact velocity, it becomes possible to rewrite

$$m\ddot{x} + c\dot{x}^n + kx = 0 \tag{10}$$

which has the great advantage of capturing the damping mechanism associated with the onset of damage. When the following equation is substituted in Eq. (4):

$$P = K_0 x - cV^n \tag{11}$$

it is possible to solve for P and obtain

$$P_3^{\text{peak}} = \tfrac{1}{2}\left(-cV^n + \sqrt{c^2 V^{2n} + 8K_0 E_i}\right) = -(c/2)V^n + \sqrt{2K_0 E_i + (c^2 V^{2n})4} \tag{12}$$

which describes the peak force curve in both sub- and supercritical regimes.

The curve thus obtained is shown in Fig. 4b with optimal values of $c = 0.9$ and $n = 3.21$ obtained empirically. The optimization is obtained minimizing the error between the experimental data and the curve obtained with Eq. (12). Whereas there are many combinations of the two parameters that yield similar curves ($c = 1.54$–0.32 and $n = 3.00$–3.60), the higher the value of the damping coefficient, associated with values of the exponent near unity, the greater the discrepancy with experimental data in the subcritical regime. On the other hand, if the exponent has an excessively high value, it forces the curve to continue decreasing at higher values of impact energy, instead of reaching the constant mean value typical of the supercritical regime.

The deviation from Eq. (5) into Eq. (12) is also evident in Fig. 5a for 16- and 24-ply laminates and in Fig. 5b for a 5-in.-diam opening. Even though these configurations are more flexible and tend to fail by fiber breakage on the backface rather than delamination or compression under the impactor, the observations made for the reference configuration can still be reported. It appears, therefore, that the general mechanism by which the energy absorbed in the fracture process does not contribute to the structural response is independent of the type of damage experienced by the structure.

The ability to construct the force-energy curve by means of Eq. (12) gives the designer a powerful tool to predict the regime in which a particular impact threat stands with respect to a certain structural configuration. There are two conclusions that can be deduced by reviewing Figs. 4 and 5. First is that the peak force is strictly dependent on the value of impact energy throughout the entire range tested, up to the MSUL plateau, and therefore, caution should be used if such parameter is used to define and compare impact events. Second is that, because of its asymptotic behavior after failure, peak force cannot be used to define the state of damage in the structure.

Many research programs[7,10–12,15,16] have investigated the effect of target and impactor properties on the impact response of composite plates, but they often used peak force as the reference parameter. Plots of peak force against any other test parameter cannot be used reliably unless the peak force value is recorded at the exact same

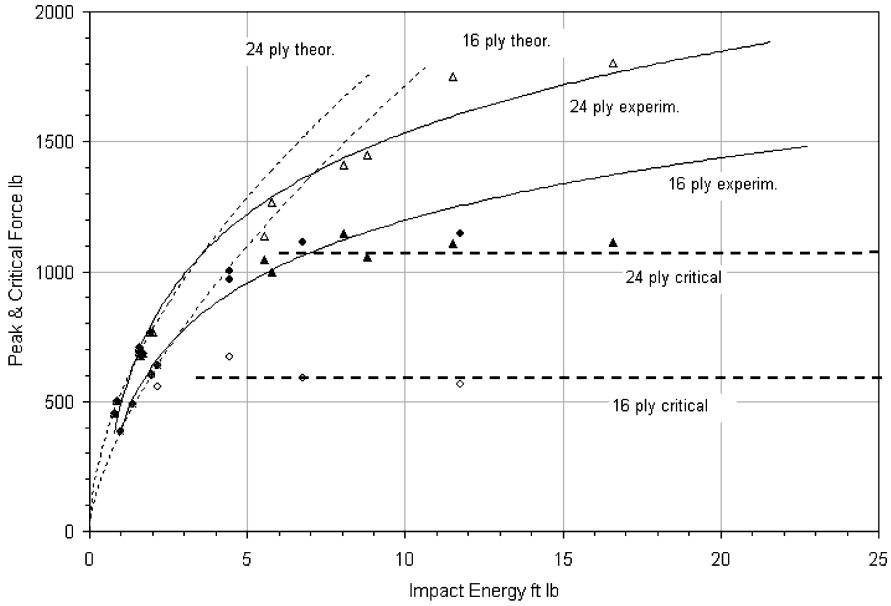

a)

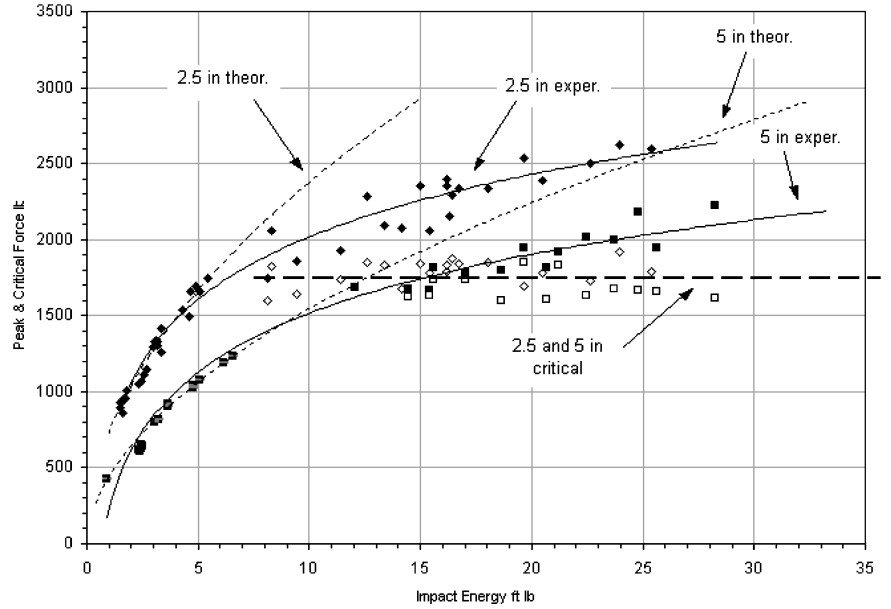

b)

Fig. 5 Similar force–energy curves observed for a) more flexible plates (16 and 24 plies thick) and b) larger support spans (5-in. diam) highlight discrepancy between Eq. (5) and experiments after introduction of damage.

value of impact energy for each test. Such a task is rather challenging; hence, comparisons between impacts on different structures should be based on other parameters that are independent of impact energy.

The dissipated energy vs impact energy is shown in Fig. 6. Again the sub and supercritical regions are highlighted, as well as the threshold impact energy value. The critical energy value is constant with respect to impact energy, just like the critical force, which, therefore, supports the equivalency of force- and energy-based criteria. On the other hand, whereas the plot of peak force increases logarithmically, the amount of energy absorbed in the fracture process increases quadratically with impact energy; hence, impact or dissipated energy should be employed rather than peak force by a designer assigned to the task of predicting the extent of damage within a structure and assessing its residual performance.[6]

B. Contact Duration and Coefficient of Restitution Curves

An elastic impact test[23,24] can be used to obtain information on the properties of the material/structure combination, such as coefficient of restitution (COR) and contact duration, which, unlike peak force, are independent of impact energy, as long as no failure occurs in the laminate. The contact duration shown in Fig. 7 and the COR in Fig. 8 are divided in three regions. In the first or subcritical region, contact duration is constant at around 3.5 ms for the configuration tested because it is inversely related to the effective structural stiffness K_0, which is a function of geometric and material properties of the impactor/target system. From the spring–mass model of Eq. (3), the contact duration is given by

$$t_0 = \pi\sqrt{m/K_0} \tag{13}$$

At the onset of the first delamination, contact duration exhibits a clear jump and then settles around an almost constant value of 4.5 ms for the entire second region. In the last region, it starts to increase monotonically due to the lower stiffness of the target, which is progressively experiencing damage. It is then possible to deduce that impulse duration relates very well with the instantaneous stiffness of the plate undergoing fracture and, hence, can be used to describe accurately the damage state in the structure.

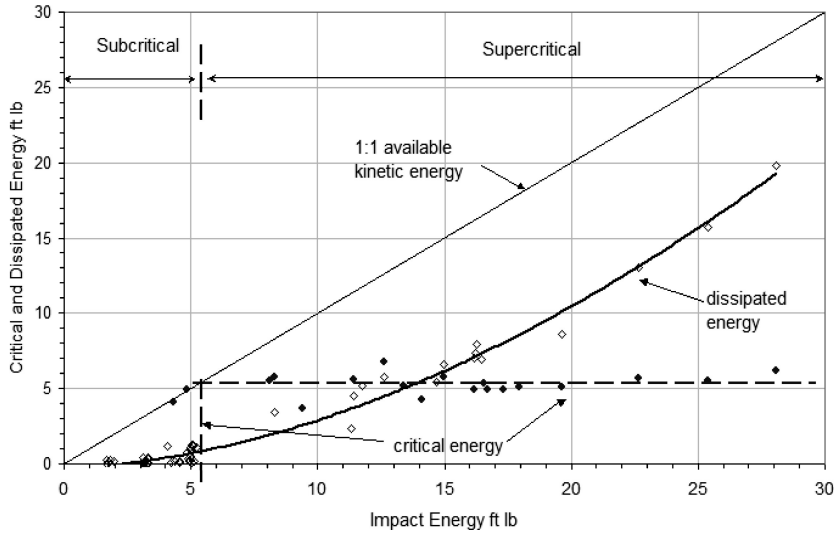

Fig. 6 Critical and dissipated energy as a function of impact energy.

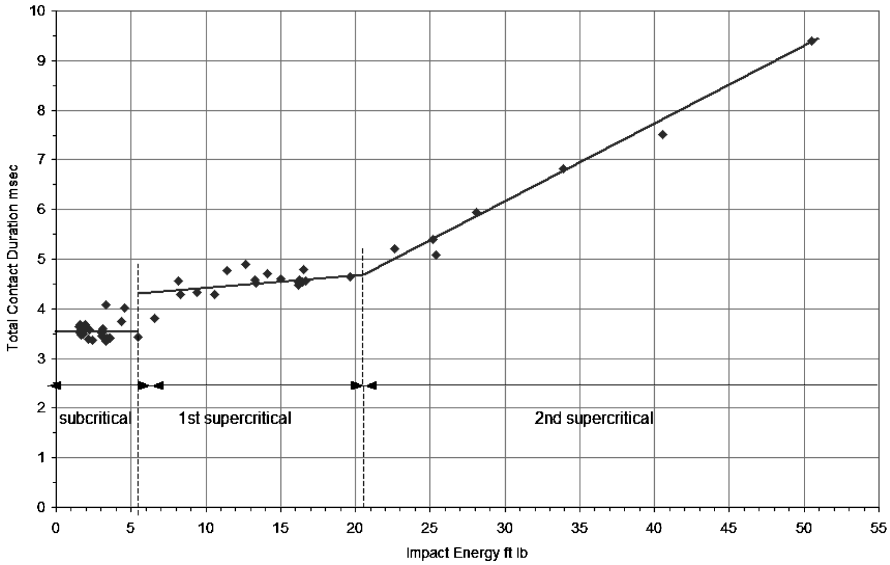

Fig. 7 Total contact duration variation with impact energy; evident are the three stages of damage: 1) none, 2) matrix delamination and splitting, and 3) fiber breakage.

Similarly, the COR oscillates in the subcritical regime around a constant value of 0.95 for the present configuration and is an indicator of the energy dissipated in frictional and vibrational damping at the supports and within the laminate (Fig. 8). The COR of an immovable target can be equivalently defined as the ratio of the exit to the incident velocity, or the square root of the ratio of the exit to the incident energy:

$$\mathrm{COR} = v_{\mathrm{out}}/v_{\mathrm{in}} = \sqrt{E_{\mathrm{out}}/E_i} \tag{14}$$

At the onset of delamination damage, it follows a sharp drop, and it becomes constant again at a value around 0.75. In the third region, at the onset of fiber breakage, the COR decreases further, but now it does not plateau around a certain value, and yet it follows a progressively decreasing power law curve.

From Figs. 7 and 8, it is then possible to conclude that the supercritical regime can be divided in two regions, the first characterized by matrix damage in the form of splitting and delamination and the second dominated by extensive fiber breakage, as determined experimentally.[6,24,31] In this latter region, the dissipated energy increases at a much faster rate than the kinetic energy available, and eventually, at the perforation threshold, the two quantities will coincide.

The discontinuous behavior of the COR plot suggests that the dissipated energy curve can also be divided in three regimes, namely, elastic response, delamination damage, and fiber breakage. Because $E_{\mathrm{out}} = E_i - E_D$, it is possible to write

$$E_D = E_i(1 - \mathrm{COR}^2) \tag{15}$$

In the subcritical regime (0–5.6 ft · lb), where the COR is constant, it is possible to obtain

$$E_D = E_i(1 - \eta^2) \tag{16}$$

and because $\eta = 0.94$, $E_D = 0.12E_i$. In the first stage of the supercritical regime (up to 20 ft · lb), where the COR decreases linearly:

$$E_D = E_i\left\lfloor 1 - (\lambda E_i + a)^2 \right\rfloor \cong E_i(1 - a^2) \tag{17}$$

where $\lambda = -0.0028$, $a = 0.80$, and, therefore, $E_D = 0.64E_i$. In the second supercritical regime (beyond 20 ft · lb), where the COR decreases according to a power law equation, it is possible to obtain

$$E_D = E_i\left\lfloor 1 - \left(\gamma E_i^{\frac{1}{2}} + b\right)^2 \right\rfloor \tag{18}$$

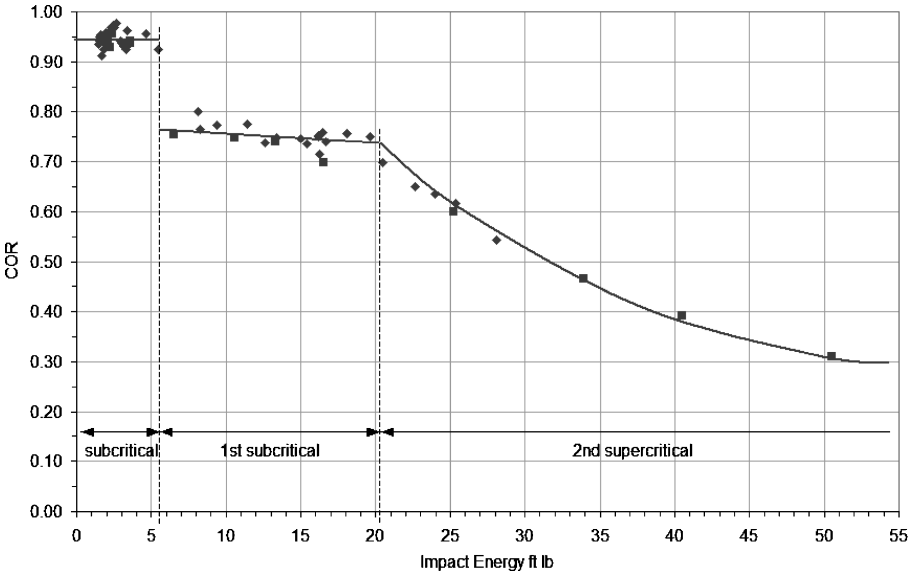

Fig. 8 Coefficient of restitution variation with impact energy; evident are the three stages of damage: 1) none, 2) matrix delamination and splitting, and 3) fiber breakage.

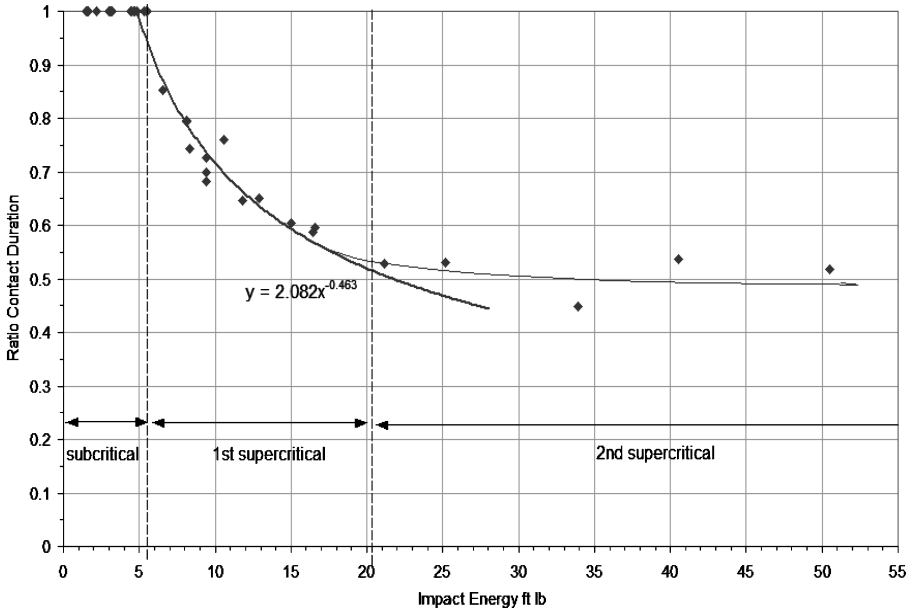

Fig. 9 Normalized contact duration, obtained by elastic testing a specimen before and after introducing damage, yields a CAI-type curve if plotted against the impact energy value that introduced damage in the preceding test.

where $\gamma = -0.22$ and $b = 1.85$. These equations, consistent with the observations made by Liu and Raju,[31] support the conclusions that the dissipated energy curve, even though quadratic in appearance, can be divided in three regimes, having different rates of dissipation of kinetic energy. Also, because dissipated energy is a direct indication of the damage state accumulated in the structure, it is possible to conclude that there exist specific thresholds for the different failure mechanisms.

C. Residual Stiffness Curve

Because of the great deal of information on structural response that can be obtained from an elastic impact test, it is useful to perform this type of test on specimens that have been previously impact damaged, to assess the state of damage below the surface and, possibly, estimate the residual performance. For a postdamage elastic impact test, a lower peak force, longer impulse duration, and higher COR are observed, which are direct consequences of the lower laminate stiffness.

The adoption of a test matrix that comprises three consecutive impact tests for each specimen allows for great insight in the structural behavior of a composite target. The importance of the first and last tests, which are nondestructive (elastic) in nature, is to record the pristine and damaged values of contact duration and COR. The second test, performed at different impact energy levels, has the purpose of introducing a progressively increasing amount of damage in the specimen.

An intriguing phenomenon is reported to occur for the COR, that is, the value of the damaged specimen is higher than that of the pristine specimens. It is strongly believed that such an increase is due to two concurrent factors, namely, a trampoline effect and a lower impact energy dissipation in global deformation that the damaged, hence, more compliant, structures exhibit. On the other hand, the ratio of COR yields limited insight in damage assessment because of the limited range of values that it can assume between the pristine (0.95) and the damaged values (at most, unity).

The ratio of pristine, t_0, to damaged t_D, impulse duration proves to be a very reliable indicator of residual laminate performance. The curve shown in Fig. 9 has the same significance as the curves obtained by CAI-type tests,[12,19,26] and it has the advantage of saving the burden of performing these time-consuming tests. The normalized contact duration curve shows that

$$t_0/t_D = (K_D/K_0)^{\frac{1}{2}} = (E_C/E_i)^{\alpha} \tag{19}$$

where E_C is the threshold impact energy of 5.25 ft · lb (7.12 J), E_i is impact energy, K_0 and K_D are the pristine and damaged values of the transverse stiffness, respectively, and α is an experimental parameter. The value of the damaged stiffness can be used a posteriori in Eq. (6) to extrapolate the force–energy curve. Similar curves can be constructed for 24- and 40-ply laminates, as well as for larger support spans (Figs. 10a and 10b). Although laminate thickness appears to shift the curve (depending on the relative value of E_C), without affecting its rate of decay (exponent α), the support span seems to influence directly the degradation mechanism of the plate and its residual performance (E_C and α). These findings are in good agreement with existing observations resulting from CAI tests[19,26] where laminate thickness has little effect on the normalized residual strength of a plate, whereas the unsupported area directly influences the size of damage and the structure's ability to carry compressive loads. Furthermore, Caprino and Lopresto[32] obtained a similar expression for the residual tensile tension after impact (TAI) performance of impacted panels:

$$\sigma_D/\sigma_0 = (E_C/E_i)^{\alpha} \tag{20}$$

where σ_D and σ_0 are the damaged and pristine strength, respectively. Even though TAI strength is mostly dependent on fiber damage, and CAI strength is directly related to the transverse stiffness of the damaged plate[26] because of the characteristic failure mechanism consisting of sublaminate buckling of delaminated areas, Eq. (19) for normalized contact duration bears a striking resemblance to Eq. (20) for normalized strength. The present result gives the ability to infer the residual properties that a damaged specimen will sustain at any impact energy level by simply knowing the value of the threshold impact energy necessary for the onset of delamination. The ratio of contact duration appears, therefore, to be a direct and viable tool

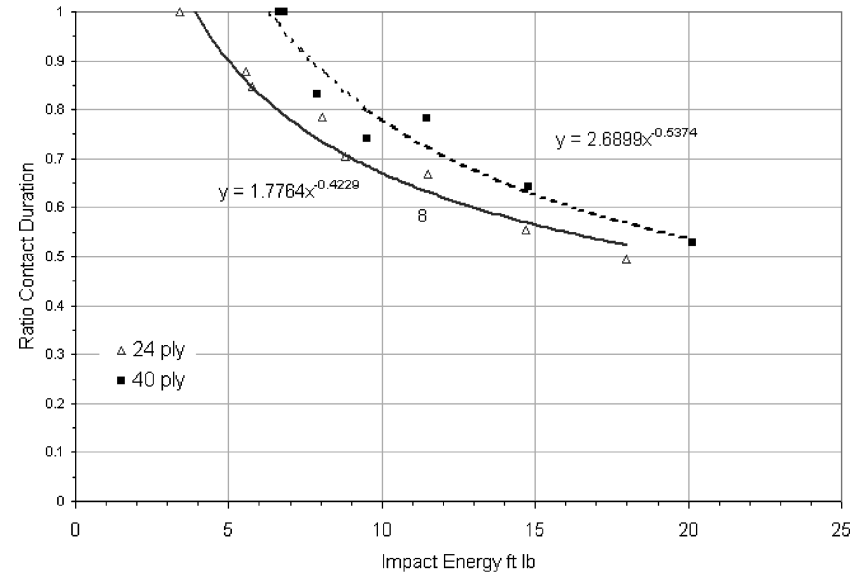

a)

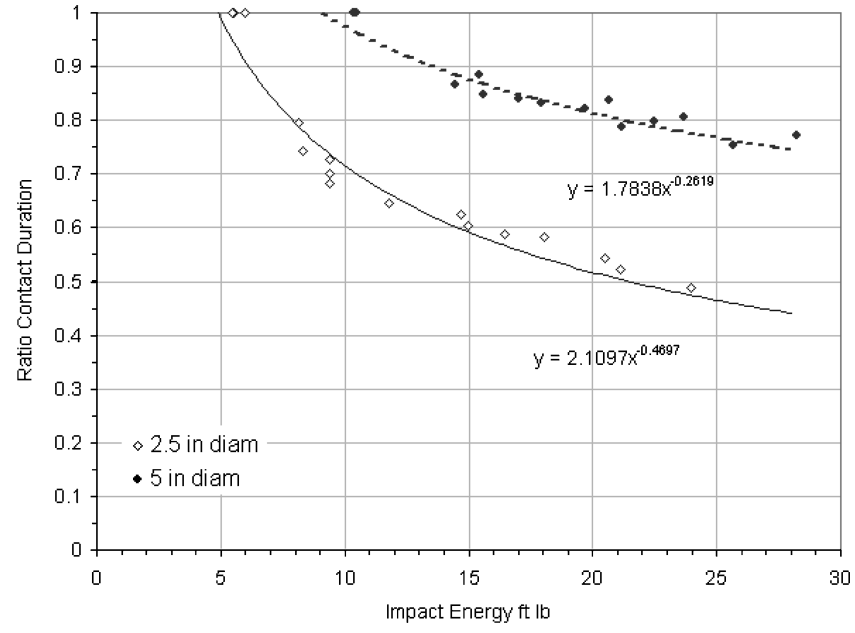

b)

Fig. 10 Residual stiffness ratio plots for a) thinner laminate and b) larger aperture size yield similar trends.

to assess the damage tolerance of the structure, without having to perform expensive and time-consuming tensile or CAI tests.

V. Conclusions

The prediction of the peak force–energy curve based on the well-accepted spring–mass model ceases to be accurate beyond the damage initiation threshold; hence, peak force should be used very carefully in parametric investigations and can result in limited use for assessing the state of damage in the so-called damage maps. To account for the instantaneous state of damage within the structure, the existing model is modified with the introduction of absorbed energy and progressive stiffness degradation. In particular, the introduction of a nonlinear viscous damper to simulate the effect of damage greatly improves the accuracy of the model in the regime beyond the structural integrity threshold.

The adoption of a test matrix comprising three consecutive impact tests for each specimen allows for greater insight in the structural behavior of composite targets than conventionally obtained. The importance of the first and last tests, which are nondestructive in nature, is to record the pristine and damaged values of contact duration and COR. The second test, performed at different impact energy levels, is to introduce a progressively increasing amount of damage in the specimen. Both contact duration and COR are shown to be viable tools for interpreting the impact response of composite plates, being constant over a wide range of impact energies and decreasing in finite increments with impact energy in the supercritical regimes, according to the progressive types of failure mechanisms. The normalized contact duration (ratio of pristine to damaged) obtained by elastic impact testing can be used to assess the residual performance and damage tolerance of a composite laminate because it promises to be a viable alternative to the costly and tedious CAI strength testing.

Acknowledgments

The authors express their appreciation to D. Jacobson (C. G. Co.) for continuously supporting the research. They also express their gratitude to T. K. O'Brien (U.S. Army Research Laboratories–Vehicle Technology Directorate) for his mentoring and constructive conversations and W. C. Jackson (U.S. Army Research Laboratories, NASA Langley Research Center) for the long and insightful reviews of the study. Per aspera astra ad ulteriora.

References

[1]"Test Method for Measuring the Damage Resistance of a Fiber Reinforced Polymer-Matrix Composite to a Concentrated Quasi-Static Indentation Force," American Society for Testing and Materials, Rept. ASTM D6264-98, 1998.

[2]Jackson, W. C., and Poe, C. C., "The Use of Impact Force as a Scale Parameter for the Impact Response of Composite Laminates," NASA TM 104189, Jan. 1992.

[3]Sjöblom, P., "Simple Design Approach Against Low Velocity Impact Damage," *32nd International Society for Advancement of Material and Process Engineering Symposium*, 1987, pp. 529–539.

[4]Aleszka, J. C., "Low Energy Impact Behavior of Composite Panels," *Journal of Testing and Evaluation*, Vol. 6, No. 3, 1978, pp. 202–210.

[5]Belingardi, G., and Vadori, R., "Low Velocity Impact Tests of Laminate Glass Fiber Epoxy Matrix Composite Material Plates," *International Journal of Impact Engineering*, Vol. 27, 2002, pp. 213–222.

[6]Delfosse, D., and Poursartip, A., "Energy-Based Approach to Impact Damage in CFRP," *Composites*, Pt. A, Vol. 28A, 1997, pp. 647–655.

[7]Nettles, A. T., and Douglas, M. J., "A Comparison of Quasi-Static Indentation to Low-Velocity Impact," NASA TP-210481, Aug. 2000.

[8]Hahn, H. T., Mitrovic, M., and Turkgenc, O., "The Effect of Loading Parameters on Fatigue of Composite Laminates," Dept. of Transportation, Rept. DOT/ FAA/AR-99/22, June 1999.

[9]Cartie, D. D. R., and Irving, P. E., "Effect of Resin and Fibre Properties on Impact and Compression After Impact Performance of CFRP," *Composites*, Pt. A, Vol. 33, 2002, pp. 483–493.

[10]Schoeppner, G. A., and Abrate, S., "Delamination Threshold Loads for Low Velocity Impacts on Composite Laminates," *Composites*, Pt. A, Vol. 31, 2000, pp. 903–915.

[11]Ambur, D., and Kemmerly, H. L., "Influence of Impactor Mass on the Damage Characteristics and Failure Strength of Laminated Composite Plates," AIAA Paper 98-1784, 1998.

[12]Ambur, D., and Starnes, J. H., "Effect of Curvature on the Impact Damage Characteristics and Residual Strength of Composite Plates," AIAA Paper 98-1881, 1998.

[13]Prasad, C. B., Ambur, D. R., and Starnes, J. H., "Response of Laminated Composite Plates to Low Speed Impact by Different Impactors," *AIAA Journal*, Vol. 32, No. 6, 1994, pp. 1270–1277.

[14]Ambur, D. R., Starnes, J. H., and Prasad, C. B., "Low Speed Impact Damage Initiation Characteristics of Selected Laminated Composite Plates, *AIAA Journal*, Vol. 33, No. 10, 1995, pp. 1919–1925.

[15]Wardle, B. L., and Lagace, P. A., "On the Behavior of Composite Shells Under Transverse Impact and Quasi Static Loading," MIT Industrial Liaison Program Rept., 6-8-98, Massachusetts Inst. of Technology, Cambridge, MA, 1998.

[16]Wardle, B. L., and Lagace, P. A., "Importance of Instability in Impact Response and Damage Resistance of Composite Shells," *AIAA Journal*, Vol. 35, No. 2, 1997, pp. 389–396.

[17]Wardle, B. L., and Lagace, P. A., "Behavior of Composite Shells Under Transverse Impact and Quasi-Static Loading," *AIAA Journal*, Vol. 36, No. 6, 1998, pp. 1065–1073.

[18]Zhou, G., "Damage Mechanics in Composites Laminates Impacted by a Flat Ended Impactor," *Composites Science and Technology*, Vol. 54, 1995, pp. 267–273.

[19]Zhou, G., "Effect of Impact Damage on Residual Compressive Strength of Glass-Fibre Reinforced Polyester (GFRP) Laminates," *Composite Structures*, Vol. 35, 1996, pp. 171–181.

[20]Found, M. S., and Howard, I. C., "Single and Multiple Impact Behaviour of a CFRP Laminate," *Composite Structures*, Vol. 32, 1995, pp. 159–163.

[21]Scarponi, C., Briotti, G., Barboni, R., Marcone, A., and Iannone, M., "Impact Testing on Composites Laminates and Sandwich Panels," *Journal of Composites Materials*, Vol. 30, No. 17, 1996, pp. 1873–1911.

[22]Liu, D., Raju, B. B., and Dang, X., "Size Effects on Impact Response of Composite Laminates," *International Journal of Impact Engineering*, Vol. 21, No. 10, 1998, pp. 837–854.

[23]Lifschiz, J. M., Gov, F., and Gandelsman, M., "Instrumented Low-Velocity Impact of CFRP Beams," *International Journal of Impact Engineering*, Vol. 16, No. 2, 1995, pp. 201–215.

[24]Feraboli, P. J., Ireland, D. R., and Kedward, K. T., "On the Role of Force, Energy and Stiffness in Low Velocity Impact Events," 18th American Society for Composites Technical Conf., Oct. 2004.

[25]Bland, P. W., and Dear, J. P., "Observations on the Impact Behavior of Carbon–Fibre Reinforced Polymers for the Qualitative Validation of Models," *Composites*, Pt. A, Vol. 32, 2001, pp. 1217–1227.

[26]Kan, H. P., Cordero, R., and Whitehead, R. S., "Advanced Certification Methodology for Composite Structures," Dept. of Transportation, Rept. DOT/FAA/AR-96/111, April 1997.

[27]Kan, H. P., "Enhanced Reliability Prediction Methodology for Impact Damaged Composite Structures Advanced Certification Methodology for Composite Structures," Dept. of Transportation, Rept. DOT/FAA/AR-97/79, Oct. 1998.

[28]Feraboli, P. J., and Kedward, K. T., "A New Composite Structure Impact Performance Assessment Program," 19th American Society for Composites/American Society for Testing and Materials Technical Conf., Oct. 2003.

[29]Abrate, S., "Modeling of Impacts on Composite Structures," *Composite Structures*, Vol. 51, 2001, pp. 129–138.

[30]Ireland, D. R., "Procedures and Problems Associated with Reliable Control of the Instrumented Impact Test," American Society for Testing and Materials, Rept. ASTM STP 563, Philadelphia, 1974.

[31]Liu, D., and Raju, B., "Effects of Bending–Twisting Coupling on Impact Resistance of Composite Laminates," 18th ASC Technical Conf., 2003.

[32]Caprino, G., and Lopresto, V., "The Significance of Indentation in the Inspection of Carbon Fibre Reinforced Plastic Panels Damaged by Low-Velocity Impact," *Composites Science and Technology*, Vol. 60, 2000, pp. 1003–1012.

B. Sankar
Associate Editor